

RETRACTED ARTICLE: A stabilizer-free and organic solvent-free method to prepare 10-hydroxycamptothecin nanocrystals: in vitro and in vivo evaluation

Xiaofeng Yang¹
Yingying Liu^{1,2}
Yanna Zhao¹
Meihua Han¹
Yifei Guo¹
Haixue Kuang²
Xiangtao Wang¹

¹Key Laboratory of Bioactive Substances and Resources Utilization of Chinese Herbal Medicine, Institute of Medicinal Plant Development, Chinese Academy of Medical Sciences and Peking Union Medical College, Beijing, ²School of Pharmacy, Heilongjiang University of Traditional Chinese Medicine, Harbin, People's Republic of China

Abstract: 10-Hydroxycamptothecin (10-HCPT) is a promising anticancer drug with a wide spectrum of antitumor activities. Due to its poor solubility, the carboxylate form that shows high water solubility but minimal anticancer activity and pharmacokinetic defects is used in the marketed 10-HCPT injections, resulting in its limited clinical application. To develop a simple, safe, and highly effective drug delivery system, a modified acid-base microprecipitation combined with a high-pressure homogenization technique was adopted to prepare 10-HCPT nanocrystals. Neither organic solvents nor stabilizers were employed throughout the preparation process. The in vitro and in vivo performances of the resulting 10-HCPT nanocrystals were investigated systematically. The nanocrystals were spherical with a small size of ~130 nm, and the actual drug-loading content was as high as 75%. The nanocrystals displayed a sustained release pattern and were proven to have higher cell uptake and antiproliferative activity than the 10-HCPT injections. The 10-HCPT nanocrystals also showed enhanced drug accumulation in tumors and better anticancer efficacy in 4T1-bearing mice. In summary, the 10-HCPT nanocrystals prepared in this study seem to be a promising delivery system for a new form of 10-HCPT dosages.

Keywords: 10-hydroxycamptothecin, drug delivery, poloxamer 188, high drug payload, 4T1-bearing mice

Introduction

10-Hydroxycamptothecin (10-HCPT) is a type of anticancer alkaloid isolated from the seeds of a native tree in People's Republic of China, and it is the most potent compound among the 20 isolated monomers.¹ 10-HCPT can selectively inhibit topoisomerase I and subsequently interfere with DNA replication,² which initiates cell death in a broad range of cancer cells.³ 10-HCPT is usually converted to its sodium salt in the marketed injections to resolve the issue of insolubility,⁴ and in this way, the E-ring of 10-HCPT must be opened. However, an analysis of the structure–activity relationship shows that the E-ring of 10-HCPT is essential for its antitumor activity,⁵ and some side effects would be produced by the opening of the E-ring.⁶

To overcome the aforementioned limitations, new drug delivery systems were developed for 10-HCPT, particularly nanodrug delivery systems, such as niosomes,⁷ micelles,^{8,9} emulsions,¹⁰ liposomes,¹¹ nanoparticles,^{12,13} and polymorphic nanoparticle dispersions.¹⁴ They have been shown to achieve success to some extent. Nanotechnology increased the 10-HCPT dissolution rate and enhanced its absorption and bioavailability. Furthermore, nanodrugs can accumulate in certain solid tumors by the so-called enhanced permeation and retention effect¹⁵ to improve the therapeutic efficacy and reduce side effects.

Correspondence: Xiangtao Wang
Key Laboratory of Bioactive Substances and Resources Utilization of Chinese Herbal Medicine, Institute of Medicinal Plant Development, Chinese Academy of Medical Sciences and Peking Union Medical College, No. 31, Malianwa North Road, Haidian District, Beijing 100193, People's Republic of China
Tel +86 10 5783 3266
Email xtaowang@163.com

Haixue Kuang
School of Pharmacy, Heilongjiang University of Traditional Chinese Medicine, No 24, Heping Road, Xiangfang District, Harbin 150040, People's Republic of China
Email hxkuang56@163.com

Among these delivery systems, nanocrystals have received a great amount of attention because of their high drug loading, stability, and delivery in vivo. Generally, preparation techniques for nanocrystals can be divided into two categories: bottom-up and top-down.¹⁶ Nanocrystals can be prepared directly by crystallization or precipitation (bottom-up) or by reducing the size of the crystals to the nanometer range through high-energy processes (top-down). The microprecipitation and high-energy approaches can also be combined to exploit the advantages of these crystals, such as small diameter (<200 nm) and low polydispersity.^{17,18}

Usually, the microprecipitation process needs an organic solvent to dissolve 10-HCPT, which is likely to cause environmental pollution and safety concerns over the residual solvent.¹⁹ Several methods were used mainly to solve the problem of the toxic residual organic solvent. The supercritical antisolvent technique is one type of effective method using a special instrument.²⁰ Another method is to replace the toxic organic solvents with low toxicity or nontoxic solvents; however, a water/organic phase over 25:1 is required to obtain particle size <200 nm, leading to a huge volume of water due to the poor solubility of 10-HCPT.¹³ In a recent report, I-PEG was used to form a liquid compound with 10-HCPT and was then used to prepare HCPT-loaded human serum albumin nanoparticles through an unconventional approach. But this method was complex and time-consuming. Insoluble 10-HCPT can be easily dissolved into a basic solution by the opening of its lactone ring and then be precipitated from the bulk solution by reversibly closing its lactone ring upon acidification. This property makes it possible to prepare 10-HCPT nanosuspensions or nanocrystals using an alkali dissolution and acid precipitation method. Zhao et al²² used acid precipitation combined with a high-pressure homogenization technique to obtain 10-HCPT nanosuspensions, and the drug loading was 100% even without considering that 10% mannitol was added as cryoprotective agent for lyophilization. After constitution with 5% glucose, the resulting mean diameter increased to >350 nm, which was still too large for drug delivery to tumor. Therefore, more work must be performed to achieve solvent-free preparations, small particle size (<200 nm), and high drug payloads.

In the current work, 10-HCPT nanocrystals were prepared using a modification of the acid-base microprecipitation combined with a high-pressure homogenization technique. The mean particle size was only 130 nm, with polydispersity index (PDI) of 0.13, and the drug payload of the final lyophilized final product reached 75%. Organic solvent was not used and stabilizer was also not needed throughout the preparation process. Poloxamer 188 (P188), which was approved by the US

Food and Drug Administration as a pharmaceutical adjuvant for intravenous injections, was selected as the cryoprotective agent. To evaluate the drug delivery system developed in this study, in vitro characterizations, antiproliferative activity and cellular uptake characteristics, in vivo pharmacokinetic analysis, tissue distribution tests, and antitumor activity were investigated.

Materials and methods

Materials

10-HCPT (99.5%) was purchased from Beijing Ouhe Technology Ltd (Beijing, People's Republic of China). 10-HCPT injections were obtained from Shenghe Pharmaceutical Ltd (Sichuan, People's Republic of China). P188 (injection grade) and 3-(4,5-dimethylthiazole-2-yl)-5-diphenyl-4-azole nitrogen bromine salt (MTT), Dulbecco's Modified Eagle Medium, fetal bovine serum (FBS), and RIPA Lysis Buffer were purchased from Sigma-Aldrich Co. (St Louis, MO, USA). Acetonitrile and methanol (both high performance liquid chromatography (HPLC) grade) were purchased from Thermo Fisher Scientific (Waltham, MA, USA). Roswell Park Memorial Institute-1640, 5% trypsin, and penicillin and streptomycin were purchased from Thermo Fisher Scientific.

Other reagents used in the experiments were bought from Sinopharm Chemical Reagent Ltd (Beijing, People's Republic of China). The water used throughout the experiments was deionized, and all other reagents were of analytical grade. All solutions used in HPLC analysis were filtered using 0.45 µm membrane filter.

Animals and cell culture

Female BALB/c mice (SPF grade, 6–8 weeks, 18–22 g) were obtained from Vital River Laboratory Animal Technology Ltd (Beijing, People's Republic of China). All animal experiments were performed in accordance with the Regulations for Animal Experiments and Guidelines for Ethical as defined by The Institute of Medicinal Plant Development (Beijing, People's Republic of China). The ethics committee/institutional review board of the Institute of Medicinal Plant Development (Beijing, People's Republic of China) granted ethical approval for this study.

All of the tumor cells used in the experiments were obtained from the Cell Culture Center of Chinese Academy of Medical Science, Beijing, People's Republic of China. The A549 cells were cultured in Dulbecco's Modified Eagle Medium (high glucose), and the other cells were cultured in Roswell Park Memorial Institute-1640 medium, supplemented with 10% FBS, 1% penicillin and streptomycin. The cells were incubated in a 37°C incubator with 5% CO₂ in air and subcultured every 3 days with 0.25% trypsin.

HPLC analysis of 10-HCPT

A reverse-phase HPLC (Ultimate 3000; Thermo Fisher Scientific) system was utilized for determination of 10-HCPT concentrations. A Symmetry C18 column (250×4.6 mm²; Waters, Milford, MA, USA) was employed. The mobile phase was composed of 28% acetonitrile and 72% water with acetic acid (0.1%). The flow rate was set at 0.8 mL/min, and the column temperature was 30°C. The detection was performed by measuring the UV-vis absorption at 384 nm.

A higher sensitivity and lower detection limit were required to detect the concentrations of 10-HCPT in biological samples; therefore, a fluorescence detector (DIONEX, Sunnyvale, CA, USA; λ_{ex} 375 nm and λ_{em} 435 nm) was used. The other conditions were similar to those used in the ultraviolet detection method.

Preparation of 10-HCPT nanocrystals

10-HCPT nanocrystals were prepared using a previously reported method, with some modifications.¹² Briefly, 10-HCPT powder (25 mg) was dissolved in 2 mL of 0.1 M sodium hydroxide solution. Then, 0.1 M hydrochloric acid (a total of 2 mL) was slowly added to the alkaline 10-HCPT solution with rapid shaking and intense sonication (200 W, 25°C; ultrasonic cleaner; Kun Shan Ultrasonic Instruments Ltd, Kunshan, Jiangsu, People's Republic of China). With the reduction of pH, the carboxylate form of 10-HCPT was converted into the lactone form and the fine-precipitated 10-HCPT particles became crude nanocrystals. Gradient dropping was employed in our study as follows: 2 mL/min for 0.5 minutes, then 1 mL/min for 0.5 minutes, and then 0.5 mL/min for 0.6 minutes, at which time the pH was ~5.0. The resulting suspensions were centrifuged at 10,000 rpm for 10 minutes using a high-speed centrifuge (Sigma-Aldrich Co.). The remaining hydrochloric acid solution (0.2 mL) was dropped into this supernatant at a speed of 0.5 mL/min to completely convert the residual carboxylate form of 10-HCPT into lactone form and subsequent drug nanocrystals. Crude nanocrystals obtained by centrifugating twice were combined and resuspended in pure water under sonication, followed by homogenization (eight cycles at 2,000 bar and 25°C) using a JN3000 homogenizer (JNBIO Inc., Guangzhou, People's Republic of China) to obtain 10-HCPT nanocrystals.

Lyophilization and reconstitution

To enhance their chemical and physical stability, 10-HCPT nanocrystals were lyophilized for storage and subsequent use. P188 (Sigma-Aldrich Co.) was added as a

cryoprotective agent (10-HCPT and P188 with a weight ratio of 3:1). In brief, the mixture of 10-HCPT nanocrystals and P188 was pre-frozen in a refrigerator (-80°C) for 2 hours and then lyophilized in an LGJ-10B freeze-drier (Sihuan Laboratory Instruments Ltd, Sichuan, People's Republic of China) for 12 hours under the condition of -35°C and a vacuum pressure <5 Pa. A 5% glucose solution was used to reconstitute the freeze-dried samples when conducting in vivo research.

The drug loading (DL% w/w) was calculated as follows:

$$DL\% = \frac{W_{drug}}{W} \times 100\%, \quad (1)$$

where W_{drug} is the weight of drug in the formulations and W is the total weight of drugs and materials in the formulations.

Physicochemical characterizations of 10-HCPT nanocrystals

Size and zeta potential measurement

The mean particle size and PDI of the prepared 10-HCPT nanocrystals were determined by dynamic light scattering (DLS; Malvern Nano ZS; Malvern Instruments, Malvern, UK). The zeta potential (ZP) of the nanoparticles was measured with the same instrument. The nanocrystals were adjusted to a concentration of 1 mg/mL in deionized water as recommended for ZP examination. Both the particle size and ZP measurements were performed in triplicate, and each measurement was performed with 12 runs at 25°C.

Morphology observation by transmission electron microscopy

A morphological evaluation of 10-HCPT nanocrystals was conducted using transmission electron microscopy (TEM; JEM2000-FX; JEOL Ltd, Tokyo, Japan). A drop of diluted nanocrystals (100 µg/mL 10-HCPT) was applied to a 300-mesh copper net and dried in the air. Next, the nanocrystals were stained with 0.1% phosphotungstic acid for 90 seconds. Then, we observed the shape and size of the nanocrystals using TEM.

X-ray diffraction measurements

The crystal structures of 10-HCPT bulk powders, physical mixture, and 10-HCPT nanocrystals were measured. The powder X-ray diffraction (XRD) patterns were collected using a D/max 2400 X-ray diffractometer with a rotating anode (JEOL) with Cu radiation generated at 100 mA and

40 kV. The obtained data were typically collected with a step width of 0.01° and a theta scan range of 3° – 70° .

In vitro release study

To evaluate the release behavior, 10-HCPT injections, 10-HCPT nanocrystals, and 10-HCPT bulk powder were diluted with or suspended in water to a final concentration of $50 \mu\text{g/mL}$ of 10-HCPT. Approximately 2 mL of these mixtures were placed in individual dialysis bags and dialyzed against 100 mL of deionized water at $37^\circ\text{C} \pm 1^\circ\text{C}$ under constant agitation using an incubator (Jintan State Experimental Apparatus Factory, Jintan, Jiangsu, People's Republic of China). At different time intervals, 1 mL aliquots of the medium were withdrawn, and the same volume of fresh medium was added. The drug content in the dialyate was analyzed using reverse-phase HPLC.

Antiproliferative activity in vitro

Growth inhibition assays are essential for assessing the effect of a drug on tumor cells. The cellular proliferation was detected using MTT assay, which is a commonly used method. The 4T1, MCF-7, HepG2, A549, and HeLa cells in logarithmic phase were cultured in 96-well plates. Based on their different cell growth rates, 4T1, MCF-7, and HepG2 cells were plated at a density of 5,000 cells per well, and the A549 and HeLa cells were plated at densities of 2,000 and 8,000 cells per well, respectively, and incubated for 24 hours at 37°C . Then, the media were removed and different concentrations of 10-HCPT injections or 10-HCPT nanocrystals diluted in FBS-free media were added; an equal volume of FBS-free media was added to the control group. After 48-hour inhibition, the cells were treated with $20 \mu\text{L}$ of MTT solution (5 M) for an additional 4 hours. The media were then replaced with $20 \mu\text{L}$ of dimethyl sulfoxide solution, and the plates were shaken for 10 minutes to make the generated formazan dissolve completely. The mean optical density (OD) was measured at 570 nm using a plate reader (Biotek, Winooski, VT, USA). The formula used to calculate the cell inhibition rate was:

$$\text{Cell inhibition rate (\%)} = \frac{1 - \text{OD}_t}{\text{OD}_c} \times 100\%, \quad (2)$$

where OD_t is the mean OD of the test group and OD_c is the mean OD of the control group.

The 50% inhibitory concentrations (IC_{50}) of 10-HCPT injections and 10-HCPT nanocrystals were calculated using GraphPad Prism 5 software (GraphPad Software, Inc., La

Jolla, CA, USA) to reflect the antiproliferative activity in vitro.

Cellular uptake by 4T1 cells

Visualization with fluorescence microscopy

The cellular uptake was analyzed in 4T1 cells. Briefly, cells in the logarithmic phase were plated in 12-well plates and incubated at 37°C to allow the cells to attach. After 24 hours of incubation, 2 mL 10-HCPT injections or nanocrystals in different concentrations (5 , 25 , or $50 \mu\text{g/mL}$, diluted with media) were added to the wells, and the plates were incubated for 0.5, 2, or 4 hours at 37°C in a CO_2 incubator. Then the colloidal dispersion was removed after gentle aspiration, and the cells were rinsed four times with prewarmed PBS ($\text{pH } 7.4$). Cell fixation was achieved by dipping in a 4% formaldehyde solution for 20 minutes at room temperature.

The visualization study was conducted using a Delta Vision Microscopy Imaging System (Healthcare Life Sciences, Marlborough, MA, USA). The uptake of 10-HCPT by 4T1 cells was observed in the 4',6-diamidino-2-phenylindole channel ($\lambda_{\text{ex}} 390 \text{ nm}$, $\lambda_{\text{em}} 435 \text{ nm}$). The transmittance was 10%, and the exposure time was 0.08 seconds. The average fluorescence intensity was calculated under same conditions using the software provided with the system, SoftWoRx Software version 6.2 (Healthcare Life Sciences, Marlborough, MA, USA).

HPLC quantitative detection

The procedures for cell culture and incubation with agents were the same as described in "Visualization with fluorescence microscopy" section. After rinsing with PBS to remove the extracellular 10-HCPT, 0.2 mL of RIPA lysis buffer was added to each well to release the intracellular 10-HCPT. The lysate was mixed with $20 \mu\text{L}$ acetic acid followed by storage in the dark for 3 hours. Then, 1 mL of ethyl acetate was added into each well, and the mixture was vortexed vigorously for 2 minutes. After centrifugation at $10,000 \text{ rpm}$ for 10 minutes, the upper organic layer was collected and evaporated at 40°C under nitrogen. The residue was reconstituted in $200 \mu\text{L}$ of methanol, vortexed for 3 minutes, and filtrated with a $0.22 \mu\text{m}$ needle filter before HPLC analysis.

Uptake mechanism research

The influence of endocytosis inhibitors on uptake was studied to determine whether there was an endocytosis-dependent uptake mechanism. First, five different endocytosis inhibitors were diluted to an appropriate concentration with medium: 2-deoxy-D-glucose (50 mM), chlorpromazine

(30 μM), sucrose (450 mM), Hydroxypropyl- β -cyclodextrin (HP- β -CD) (10 μM), and heparin sodium (10 μM). Then, 1 mL aliquots of different endocytosis inhibitors were incubated with the 4T1 cells for 30 minutes before 50 $\mu\text{g}/\text{mL}$ of the 10-HCPT drug system was added and 1 mL of medium was added to the control group. All experiments were performed in triplicate. The remaining steps were the same as described in “HPLC quantitative detection” section.

Pharmacokinetic analysis

Twenty Sprague Dawley rats were randomly divided into two groups (10-HCPT injections group and 10-HCPT nanocrystals group) and were intravenously administered 10-HCPT injections and 10-HCPT nanocrystals, respectively, through the tail vein at a dose of 5.0 mg 10-HCPT per kilogram body weight after being fasted for 12 hours.

Blood samples (0.5 mL) were taken from the orbital plexus and collected in heparinized glass capillaries at 15 and 30 minutes and 1, 2, 4, 8, 12, and 24 hours after administration. Plasma was obtained by centrifugation at 5,000 rpm for 5 minutes. The plasma (0.2 mL) was mixed with 20 μL of acetic acid and placed in the dark for 3 hours to transform the carboxylate form into the lactone form. Then, 1.5 mL of ethyl acetate was added and the mixture was vortexed vigorously for 2 minutes. After centrifugation at 10,000 rpm for 10 minutes, the upper organic layer was collected and evaporated at 40°C under nitrogen. The residue was reconstituted in 200 μL of methanol for HPLC analysis. All parameters are calculated using WinNonlin 6.1 software (Pharsight, Inc., Mountain View, CA, USA).

Tissue distribution in 4T1-bearing mice

The 4T1 cells in logarithmic phase were diluted to 1×10^7 cells/mL with PBS (pH 7.4) and trypan digestion. Then, 0.2 mL of the 4T1 cells was injected to the right underarm of a BALB/c female mouse. When the tumor volume reached 100 mm^3 , 72 tumor-bearing mice with relatively uniform tumor volumes were randomly divided into two groups (36 mice each) and intravenously administered with 10-HCPT injections or 10-HCPT nanocrystals through the tail vein at a dose of 8.0 mg/kg. At each predetermined time interval (0.5, 1, 4, 8, 12, and 24 hours), six mice in each group were taken to collect blood samples (0.5 mL), and the animals were then killed by cervical dislocation. The heart, liver, spleen, lung, kidney, brain, and tumors were immediately removed. The plasma and tissue samples were frozen at -80°C until further analysis.

The methods used to treat the plasma samples were the same as described in Pharmacokinetic analysis (Material and methods) section. The tissue samples were rinsed with normal

saline, dried with a filter paper, and homogenized with three times the volumes of normal saline using a high-throughput tissue grinder (SCIENTZ-48; Ningbo Xingzhi Biotechnology Ltd, Ningbo, People’s Republic of China). The tissue homogenate (0.2 mL) was mixed with 20 μL of acetic acid, followed by storage in the dark for 3 hours. Then, 1.5 mL of ethyl acetate was added into the sample, and the mixture was vortexed vigorously for 2 minutes. After centrifugation at 10,000 rpm for 10 minutes, the upper organic layer was collected and evaporated at 40°C under nitrogen. The residue was reconstituted in 200 μL of methanol, vortexed for 3 minutes, and filtered with a 0.22 μm needle filter before HPLC analysis.

All parameters were calculated using WinNonlin 6.1 software (Certara, Inc., Princeton, NJ, USA).

Histological evaluation

Histological analyses were conducted to assess the tissue toxicity of the nanoparticles and injections. The group and administration methods were the same as those used for the tissue distribution analysis. Briefly, the mice from the three groups were killed 24 hours after administration and then the main tissues were immediately removed, followed by fixation in a formalin solution. The fixed tissues were embedded in paraffin for slicing. The tissue sections were photographed and analyzed.

In vivo antitumor activity in 4T1-bearing mice

The method of establishing the animal models was the same as described in “Tissue distribution in 4T1-bearing mice” section. The mice were randomly divided into five groups (ten mice each), among which three groups were intravenously injected with 10-HCPT nanocrystals (1.25, 2.5, or 5.0 mg/kg respectively), one group was intravenously administered 10-HCPT injections (5.0 mg/kg) as a positive control, and one group was intravenously injected with 0.2 mL of normal saline as a negative control. All the mice were injected every other day. Approximately 18 days after the first administration, the mice were killed and the tumors were dissected out and weighed. The tumor inhibition ratio (TIR%) was calculated as follows:

$$\text{TIR}\% = \frac{1 - W_t}{W_n} \times 100\%, \quad (3)$$

where W_n is the average tumor weight of the negative control group and W_t is the average tumor weight of the test groups.

Statistical analysis

The statistical analysis among the experimental groups was performed using an independent samples *t*-test using IBM SPSS Statistics 19 (IBM Corporation, Armonk, NY, USA). $P < 0.05$ was considered statistically significant.

Results and discussion

Preparation of 10-HCPT nanocrystals

The injection speed of the acid solution had a great effect on microprecipitation and size of the resulting 10-HCPT nanocrystals. A rapid dropping/injection speed usually led to large particles or even aggregates. Considering the time efficiency, a gradient injection pattern was adopted. For 25 mg of 10-HCPT dissolved in 2 mL of sodium hydroxide (0.1 M), a total of 2 mL of diluted hydrochloric acid (0.1 M) was needed to acidify the 10-HCPT carboxylate form. In our method, 50% of the volume of HCl solution was dropped/injected quickly at ~ 2 mL/min, which was accompanied by the color change from the dark yellow to light yellow. The injection speed had little effect on the preparation of 10-HCPT nanocrystals, as no nanocrystals formed at this stage (DLS data showing the absence of nanoparticles). Then, 25% of the volume of HCl solution was slowly added at ~ 1 mL/min, during which opalescence was observed, suggesting that 10-HCPT nanocrystals had formed. This speed could also be a little faster, but 1 mL/min was safe and reliable. Thereafter, 15% of the volume of HCl solution was added at even slower rate of ~ 0.5 mL/min to promote microprecipitation. This is a key step, and the injection speed at this stage had a critical effect on the resulting 10-HCPT nanocrystals. A higher speed would significantly increase the size of 10-HCPT nanocrystals and even occasionally result in precipitation. Since 10-HCPT nanocrystals emulsions are somewhat unstable in NaCl solution, as reported²³ and in our examination, 10-HCPT nanocrystals formed at this stage were separated from the bulk solution by centrifugation and from the NaCl salt generated during the acidification. Removal of the produced NaCl salt will improve the stability of the resulting nanocrystals and, more importantly, lead to the formation of relatively small nanoparticles in subsequent homogenization. The final 10% of the volume of HCl solution was added into the supernatant at a rate of 0.5 mL/min to guarantee the complete microprecipitation of 10-HCPT, followed by centrifugation to sediment crude 10-HCPT nanocrystals. The sediment from the two centrifugation steps was combined and resuspended in

deionized water for homogenization to obtain final product of 10-HCPT nanocrystals.

It was found that the size of resulting 10-HCPT nanocrystals rapidly increased when 15% of the volume of acid solution was injected at a higher speed. Before the first centrifugation, the size of resulting 10-HCPT particles was ~ 367 nm. However, if the final 10% of the volume of acid solution was added at this time, the resulting particles would be much larger than 1 μm or would directly precipitate. And in this case, even drastic homogenization (higher pressure and more cycles) failed to effectively reduce the size < 400 nm. So, it seems that both gradient microprecipitation and centrifugation to remove the generated sodium chloride are important in the preparation of 10-HCPT nanocrystals.

Lyophilization can significantly improve the stability of nanocrystals, thus contributing to long-term storage. However, in general, the freeze-drying process may destroy the structure of the particles, so cryoprotectant agents are usually required. In this study, P188 proved to be a good cryoprotectant similar to what was observed in a previous study.²⁴ The lyophilized 10-HCPT nanocrystals must be reconstituted into a colloid system for clinical use, and a glucose solution, one of the most commonly clinically applied media, was selected for reconstitution. As shown in Table 1, simply by resuspending the nanocrystals in a 5% glucose solution and gently shaking, the reconstituted 10-HCPT nanocrystals were restored to nearly the same size, indicating that they could be easily lyophilized and reconstituted.

To the best of our knowledge, this is the first report in which drug nanocrystals of a small size were prepared using an organic solvent-free, stabilizer-free, bottom-up procedure.

Physicochemical characterizations of 10-HCPT nanocrystals

Size, ZP, and morphology

For colloidal drug delivery systems, particle size is the primary factor that affects their in vivo biodistribution.

Table 1 Changes in the physical characteristics of 10-HCPT nanocrystals after lyophilization

Process	Size (nm)	Polydispersity index	Zeta potential (mV)
Before lyophilization	133.5 \pm 0.3	0.13 \pm 0.02	-27.1 \pm 1.36
Reconstitution with glucose	137.6 \pm 2.1	0.14 \pm 0.01	-27.2 \pm 2.32

Notes: All values are presented as mean \pm SD; n=3.

Abbreviation: SD, standard deviation.

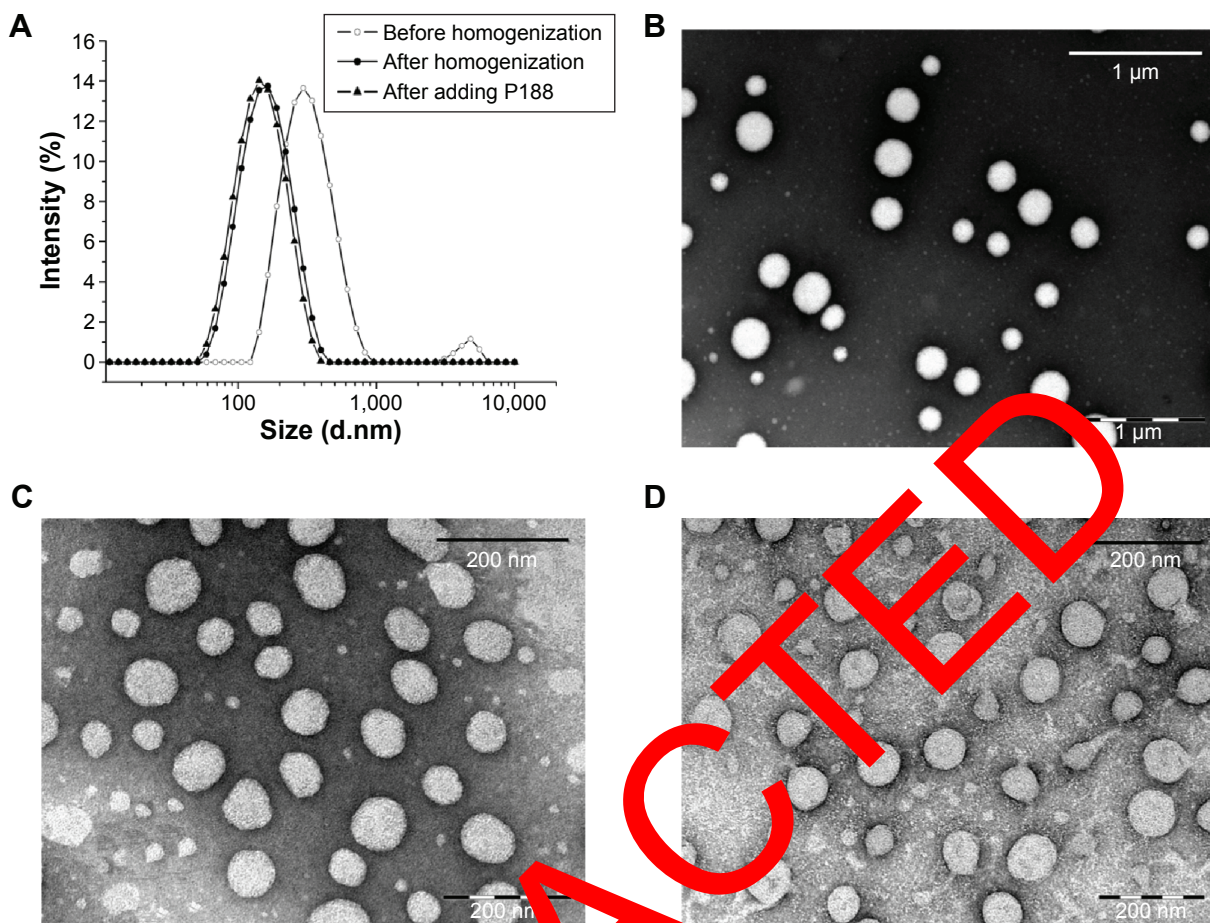


Figure 1 Particle size distribution and morphology of 10-HCPT nanocrystals.

Notes: (A) The particle sizes were measured by dynamic light scattering during the preparation process. (B) TEM micrograph of 10-HCPT nanocrystals before homogenization (scale bar, 1 μm). (C) TEM micrograph of 10-HCPT nanocrystals after homogenization (scale bar, 200 nm). (D) TEM micrograph of 10-HCPT nanocrystals after adding poloxamer 188 (scale bar, 200 nm).

Abbreviations: 10-HCPT, 10-hydroxycamptothecin; TEM, transmission electron microscopy; P188, Poloxamer 188.

A narrower particle size distribution, or smaller PDI value is also important in improving the stability of these systems by reducing Ostwald ripening effect.¹⁶ As shown in Figure 1A, the particles were large before homogenization (367.0 ± 5.1 nm), with a PDI value of 0.24 ± 0.01 . Homogenization significantly decreased the size to a mean diameter of <140 nm with a PDI value of 0.21 ± 0.02 . After lyophilization using P188 as a cryoprotector, the reconstituted 10-HCPT nanocrystals were only 133.5 ± 0.3 nm, with a narrower distribution (PDI = 0.13 ± 0.02). The TEM observations (Figure 1B–D) showed that neither homogenization nor lyophilization affected the morphology of 10-HCPT nanocrystals. The surface ZP was -27.1 ± 1.36 mV, indicating good physical stability. The actual drug-loading content was determined to be 75.0% using HPLC. Zhao et al²² did prepare 10-HCPT nanosuspensions using a similar method; however, the size was very large even in the presence of various stabilizers.

After further homogenization (15 cycles), the particles were still large (286.9 ± 6.1 nm).

The micrograph of negatively stained 10-HCPT nanocrystals (Figure 1B–D) showed that the majority of nanocrystals were spherical, which was quite different from that observed in Zhao et al's work²² using the similar preparation method. The particle size measured by DLS represents the hydration diameter, whereas TEM observes the dry particles; therefore, it is comprehensible that the size observed by TEM was a little smaller than that observed by DLS.

XRD measurements

The XRD curve of 10-HCPT bulk powders exhibited obvious diffraction peaks at 6.9° , 11.63° , 13.85° , and 25.61° (Figure 2). The diffraction peaks of 10-HCPT nanocrystals (Figure 2A) and physical mixture (Figure 2B) were nearly the same, including those peaks of 10-HCPT bulk

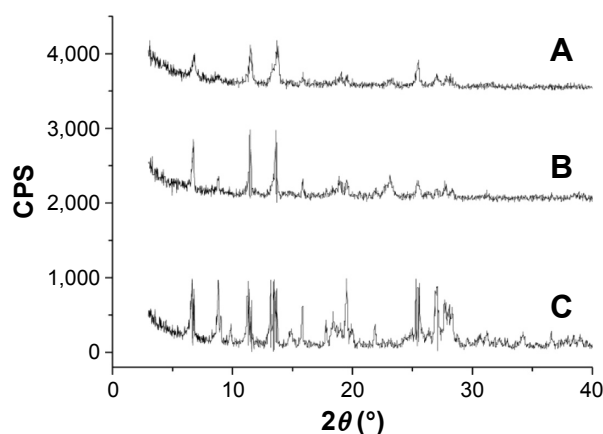


Figure 2 X-ray diffraction curves of the samples.

Notes: (A) 10-HCPT bulk powders, (B) physical mixture of poloxamer 188 and 10-HCPT, (C) 10-HCPT nanocrystals.

Abbreviations: 10-HCPT, 10-hydroxycamptothecin; CPS, counts per second.

powders, suggesting that 10-HCPT in nanocrystals was in crystalline state.

In vitro release study

The drug release behaviors of 10-HCPT injections, 10-HCPT nanocrystals, and coarse 10-HCPT suspensions were examined in neutral water over a 72-hour period. As demonstrated in Figure 3, it was not surprising that the drug was rapidly released from 10-HCPT injections, reaching 95.6% within only 5 hours. While the drug release from 10-HCPT nanocrystals was biphasic, with an initial relatively quick release followed by a steady sustained release,²⁵ the 10-HCPT powder exhibited a similar sustained release pattern, but the cumulative release was lower than

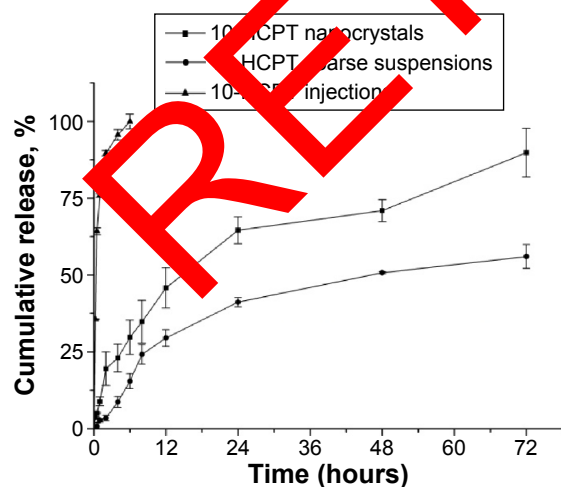


Figure 3 The release curves of 10-HCPT injections, 10-HCPT nanocrystals, and coarse 10-HCPT suspensions in water over a 72-hour period.

Note: The experiment was performed in triplicate.

Abbreviation: 10-HCPT, 10-hydroxycamptothecin.

that of 10-HCPT nanocrystals at nearly all the time intervals. The enhanced dissolution and drug release of 10-HCPT nanocrystals were mainly attributed to their higher surface area, increased surface solubility, and reduced diffusion layer thickness.²⁶

The in vitro antiproliferative activity

As shown in Figure 4A–E, both the 10-HCPT injections and nanocrystals exhibited a good inhibition of cell growth in the four tested tumor cell lines. However, 10-HCPT nanocrystals exhibited stronger inhibition than 10-HCPT injections in each case, and this was more evident in the comparison of their IC_{50} values (Figure 4F). 10-HCPT nanocrystals showed much lower IC_{50} values than 10-HCPT injections, with 4.45-, 1.10-, 0.96-, 4.2-, and 0.64-fold lower in 4T1, MCF-7, HepG2, A549, and HeLa cells, respectively. Taken together, the results seemed to show that A549, HepG2, and 4T1 cells were relatively sensitive to 10-HCPT. Moreover, the nanocrystals demonstrated the best antiproliferative improvement in 4T1 and A549 cells in contrast to injections. In 10-HCPT nanocrystals, ~100% of the drug was in lactone form, which is more effective than the carboxylate form. However, 10-HCPT injections contained only ~10% of the lactone form. Although the lactone and carboxylate forms could be mutually transformed in the culture medium (pH 7.4) during the MTT assay, the proportion of the lactone form in nanocrystals was still higher than that in the injections. For 10-HCPT injections, an equilibrium between the lactone and carboxyl forms of 10-HCPT molecules (mostly in carboxyl form at the beginning) was reached relatively quickly. However, in the case of 10-HCPT nanocrystals, it would take a much longer time to reach the final equilibrium because the drug is continuously released in the lactone form (Figure 3). This was one of the reasons that 10-HCPT nanocrystals displayed better performance. In addition, it was assumed that 10-HCPT nanocrystals may have additional advantages over the injections, such as attachment to the cell membrane and faster uptake by tumor cells.²⁷

Cellular uptake by 4T1 cells

Since 10-HCPT nanocrystals displayed the best antitumor activity improvement in 4T1 cells, this cell line was selected for the cellular uptake study. Both the carboxylate form and the lactone form of 10-HCPT exhibit the same degree of fluorescence, which can be observed through the 4',6'-diamidino-2-phenylindole channel. In the preliminary experiment, the MTT assay showed that when cells were

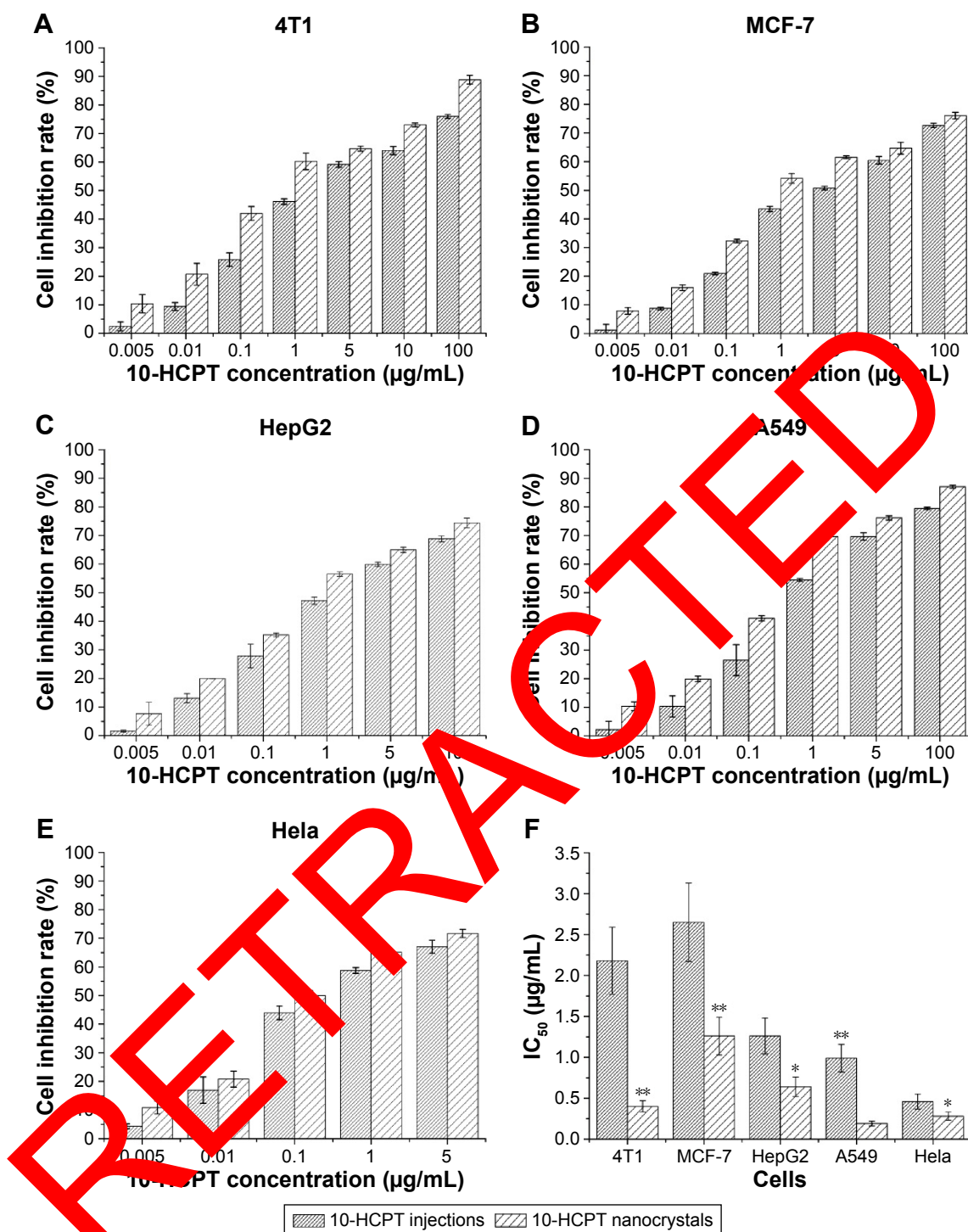


Figure 4 The in vitro antiproliferative activity of 10-HCPT.

Notes: (A–E) The inhibition rates changed as the concentration of 10-HCPT increased. (F) The IC_{50} values of 10-HCPT injections and 10-HCPT nanocrystals in different tumor cells. The results are presented as mean \pm SD, $n=6$, * $P<0.05$; ** $P<0.01$.

Abbreviations: 10-HCPT, 10-hydroxycamptothecin; IC_{50} , 50% inhibitory concentration; SD, standard deviation.

treated with the same 10-HCPT concentration of 50 μ g/mL, both 10-HCPT injections and nanocrystals groups maintained $>90\%$ cell viability after 4 hours incubation, and there was $<3\%$ difference in cell viability between the

two groups. Thus, for the cellular uptake study, the maximum concentration of the two 10-HCPT formulations was limited to no more than 50 μ g/mL, and the incubation time was limited to no more than 4 hours.

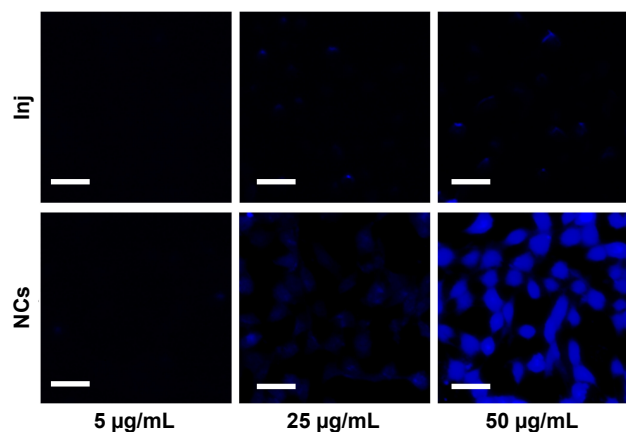


Figure 5 Confocal images of 4T1 cells incubated with different concentrations of 10-HCPT Inj and 10-HCPT NCs for 4 hours.

Note: Scale bar (30 μ m).

Abbreviations: 10-HCPT, 10-hydroxycamptothecin; Inj, injections; NCs, nanocrystals.

As observed in Figures 5 and 6, drug uptake by 4T1 cells was time- and concentration-dependent for both 10-HCPT injections and 10-HCPT nanocrystals. However, at each time interval and each concentration, the uptake of 10-HCPT nanocrystals was much higher than 10-HCPT injections, indicating that nanocrystals were superior to the injections in this regard. A semiquantitative analysis of fluorescence images (Figure 7A) showed that at 25 or 50 μ g/mL, the uptake of 10-HCPT nanocrystals by 4T1 cells was approximately tenfold ($P < 0.001$) compared with 10-HCPT injections after a 4-hour incubation.

The actual drug content absorbed in 4T1 cells was more precisely determined by HPLC, and the results displayed an even greater difference between the two formulations,

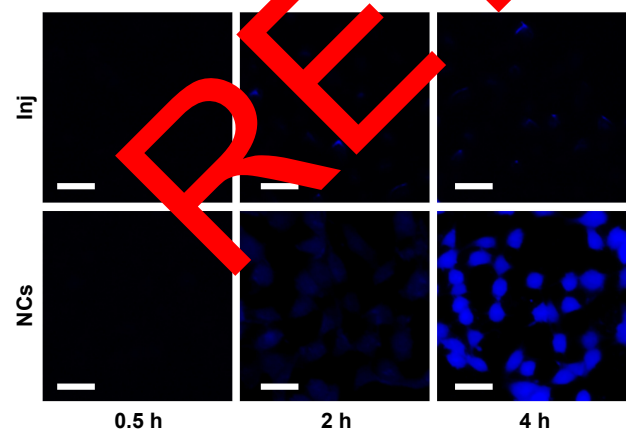


Figure 6 Confocal images of 4T1 cells incubated with 50 μ g/mL 10-HCPT Inj or 10-HCPT NCs for 0.5, 2, and 4 hours.

Note: Scale bar (30 μ m).

Abbreviations: 10-HCPT, 10-hydroxycamptothecin; Inj, injections; NCs, nanocrystals.

with significant differences ($P < 0.05$) at 5 μ g/mL and very significant differences ($P < 0.001$, by 20- to 30-fold) at 25 and 50 μ g/mL after a 4-hour incubation (Figure 7B). The time-dependent cell uptake was also quite evident, as shown in Figure 7C and D.

The antiproliferative activity is directly related to the amount of 10-HCPT that accumulates in the cells. The aforementioned results imply that the nanocrystals were more efficient at delivering the 10-HCPT molecules into cells, which confirmed our proposed hypothesis mentioned in “The in vitro antiproliferative activity” section. However, the MTT assay showed that there were no differences in the antiproliferative activity of 10-HCPT injections and 10-HCPT nanocrystals in 4 hours. It was reported that the antiproliferative activity was mediated by the internalization of nanoparticles and the subsequent release of drugs.^{27,28} Although 10-HCPT nanocrystals could be internalized more quickly by 4T1 cells, it would be more favorable for the encapsulated drugs to be released and take effect (Figure 3), and during this period the free drug from 10-HCPT injections would constantly enter the 4T1 cells even though it occurred at a relatively slower rate. This may be the major reason for the lack of difference observed in the antiproliferative activity and for significant differences in cell uptake in 4 hours as mentioned earlier.

Chlorpromazine blocks clathrin-mediated endocytosis through a mechanism by which adaptor complex 2 and clathrin are redistributed away from the plasma membrane, making clathrin unavailable for assembly at the cell surface. Hypertonic sucrose has been shown to prevent the proper assembly of clathrin lattices at the plasma membrane. As shown in Table 2, chlorpromazine, sucrose, and 2-deoxy-D-glucose could significantly inhibit the cellular uptake of 10-HCPT nanocrystals, but they had much less of an effect on the uptake of 10-HCPT injections. HP- β -CD (an inhibitor of caveolae-mediated endocytosis) and heparin sodium (an inhibitor of other types of endocytosis) had little effect on the cellular uptake of both nanocrystals and 10-HCPT injections. This showed that the increased uptake of 10-HCPT nanocrystals was mainly mediated by clathrin-dependent endocytosis.

Pharmacokinetic analysis

In our previous study,²⁹ we found that 10-HCPT nanosuspensions were not very stable in normal saline, but were stable in 5% glucose and plasma; therefore, the nanocrystals could be intravenously injected into the tail vein of rats for the pharmacokinetics study.

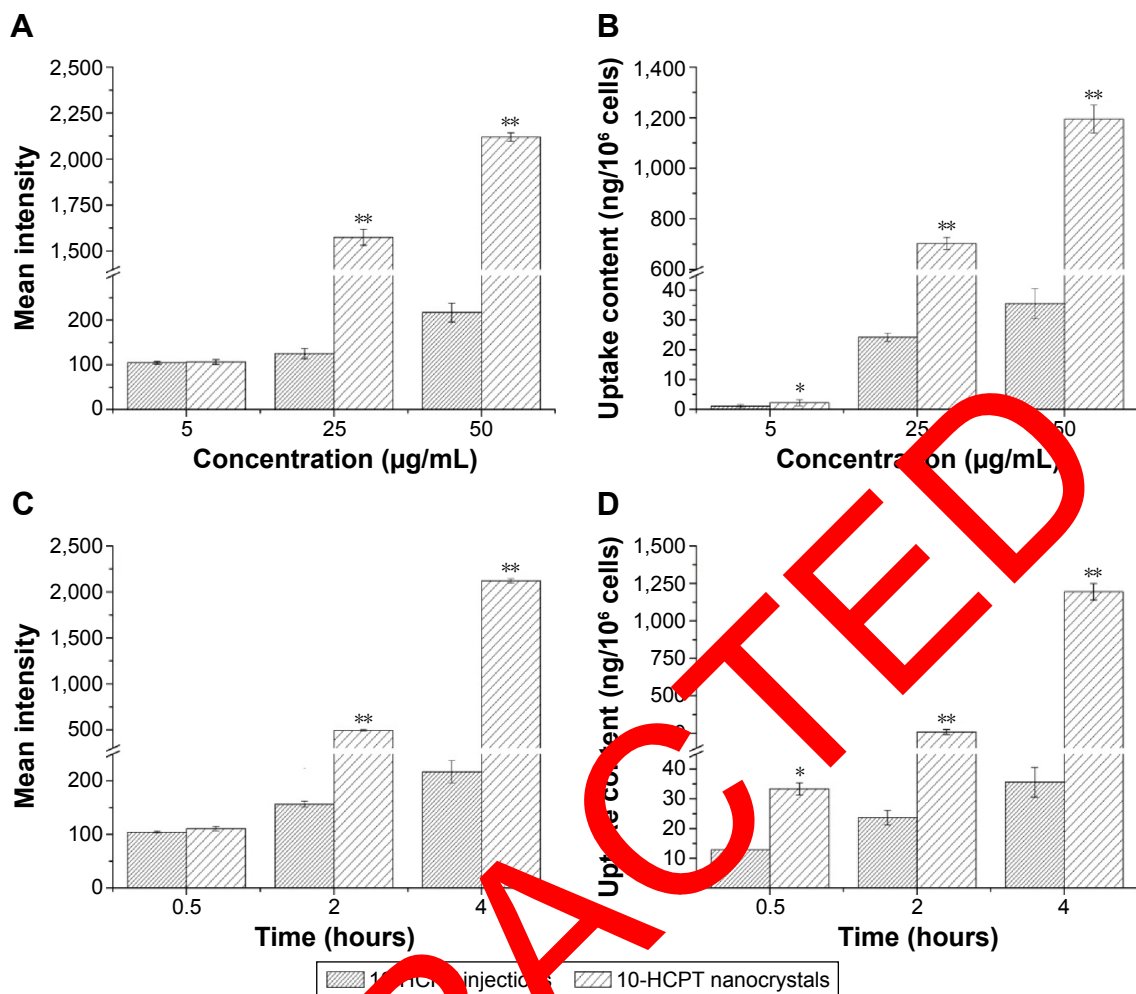


Figure 7 Mean fluorescent intensity and amount of drug taken up by HepG2 cells. **Notes:** (A, B) The cells were incubated with different concentrations of 10-HCPT for 4 hours, (C, D) or were incubated with 50 µg/mL of 10-HCPT for different times. The results are presented as mean ± SD, n=3, * $P < 0.05$, ** $P < 0.01$. **Abbreviations:** 10-HCPT, 10-hydroxycamptothecin; SD, standard deviation.

As shown in Figure 7, 10-HCPT was almost undetectable in the plasma from the injections group after 6 hours but was maintained at 186 ng/mL in the plasma from the nanocrystals group. Within 30 minutes after the intravenous

Table 2 Endocytosis inhibition rates for injections and nanocrystals after the cells were treated with different endocytosis inhibitors

Group	Endocytosis inhibition rate (%)	
	Injections	Nanocrystals
Control	NA	NA
2-Deoxy-D-glucose	3.30±0.11	24.92±0.93
Chlorpromazine	3.15±0.02	46.48±3.21
Sucrose	8.65±0.78	32.99±2.73
HP-β-CD	0.53±0.02	0.85±0.11
Heparin sodium	3.36±0.12	0.08±0.01

Notes: All values are presented as mean ± SD; n=3.

Abbreviations: SD, standard deviation; NA, not applicable; HP-β-CD, Hydroxypropyl-β-cyclodextrin.

injection, the plasma drug concentrations in the injections group were greater than those of the nanocrystals group. This was mainly due to the quick transport of 10-HCPT nanocrystals from the blood to organs such as the liver and spleen upon entering the circulatory system, which has been extensively reported.^{21,30}

The results presented in Table 3 showed that there were significant differences in the pharmacokinetic parameters between nanocrystals and injections groups. The elimination half-life of the 10-HCPT nanocrystals group was 2.98-fold as high as that of the injections group ($P < 0.001$), and the area under the curve within 24 hours (AUC_{0-24}) value was 2.81-fold as high as the injections group. Meanwhile, the mean residence time of the 10-HCPT nanocrystals group was significantly higher than the 10-HCPT injections group ($P < 0.001$), and this may contribute to the enhanced permeation and retention effect.

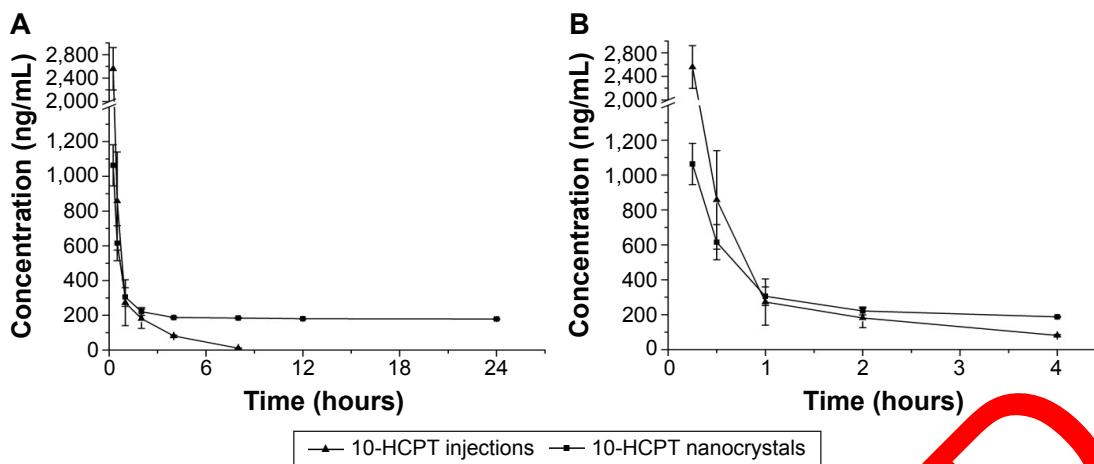


Figure 8 Concentration–time curves of 10-HCPT in Sprague Dawley rat plasma after an intravenous administration of 10-HCPT injections and 10-HCPT nanocrystals. **Notes:** The dosage was 5.0 mg/kg, n=6. **(A)** 0–24 hours, **(B)** 0–4 hours. **Abbreviation:** 10-HCPT, 10-hydroxycamptothecin.

Tissue distribution in 4T1-bearing mice

As shown in Figure 9, the biodistribution of 10-HCPT nanocrystals was significantly increased compared with 10-HCPT injections in nearly all tissues and at all time intervals after the intravenous administration.

Taking AUC_{0-24h} as an example, the biodistribution of 10-HCPT nanocrystals in the blood, heart, liver, spleen, lung, brain, and tumor were ~8.87-, 6.71-, 99.15-, 6.23-, 13.45-, 14.08-, 2.34-, and 7.25-fold as long as the 10-HCPT injections (Table 4). It was true that at the same dose, the nanocrystals delivered much more drug into the blood (7.25-fold) than injections, but even more drug was delivered into liver (99.15-fold), lung (13.45-fold), and kidney (14.08-fold). This indicated that the nanocrystals may induce more side effects than injections when the therapeutic efficacy was improved.

However, the side effects may not be as serious as it seemed from the distribution data. First, the drug content determined for the injection group was pure free drug that was mainly in the form of the more toxic carboxylate, while the drug content determined for the nanocrystals

group was composed of free drug (mainly in the lactone form) and encapsulated drug, which is not toxic before release. Second, the 10-HCPT nanocrystals distributed in the liver, spleen, and lung were mainly taken up by the monocyte/macrophage system.³¹ In addition, most of this drug will ultimately be destroyed. Third, the slow drug release of 10-HCPT nanocrystals may make the encapsulation less toxic than the same amount of free drug as 10-HCPT injections, which will instantly produce high concentrations.

Histological evaluation

As shown in Figure 10, at the same dose of 8 mg/kg, no abnormal change was observed in the mice belonging to the 10-HCPT nanocrystals group and the 10-HCPT injections group in contrast to the control group of normal saline. Significant differences may be observed at a higher dose and/or after multiple dosing. This current result indicated that at 8 mg/kg, 10-HCPT nanocrystals were safe for intravenous administration. Therefore, if the dose was selected, 10-HCPT nanocrystals may show better therapeutic efficacy than injections without increased side effect.³²

Table 3 Pharmacokinetic parameters of 10-HCPT in Sprague Dawley rat plasma after intravenous administration of 10-HCPT injections and 10-HCPT nanocrystals

Group	$t_{1/2}$ (h)	AUC_{0-24h} (ng·mL ⁻¹ ·h)	Cl (mL/h)	MRT (h)
10-HCPT Inj	0.62±0.1	1,735.9±135.5	484.99±23.4	1.4594±0.2
10-HCPT NCs	1.85±0.1**	4,867.7±46.3*	10.65±7.6**	10.35±0.2**

Notes: The results are presented as mean ± SD, n=10. *P<0.01; **P<0.001. **Abbreviations:** 10-HCPT, 10-hydroxycamptothecin; AUC_{0-24h} , area under the curve within 24 hours; Cl, clearance; Inj, injections; MRT, mean residence time; NCs, nanocrystals; $t_{1/2}$, terminal elimination half-life; SD, standard deviation.

In vivo antitumor activity in 4T1-bearing mice

The variations in tumor volume during the experimental process are depicted in Figure 11A. It can be seen that the tumors grew very fast in the negative control group, followed closely by the tumors in the 10-HCPT injections group. In the three 10-HCPT nanocrystals groups, the tumors grew more slowly and were inhibited in a dose-dependent manner. By the end of the trial, the tumor volumes of four 10-HCPT

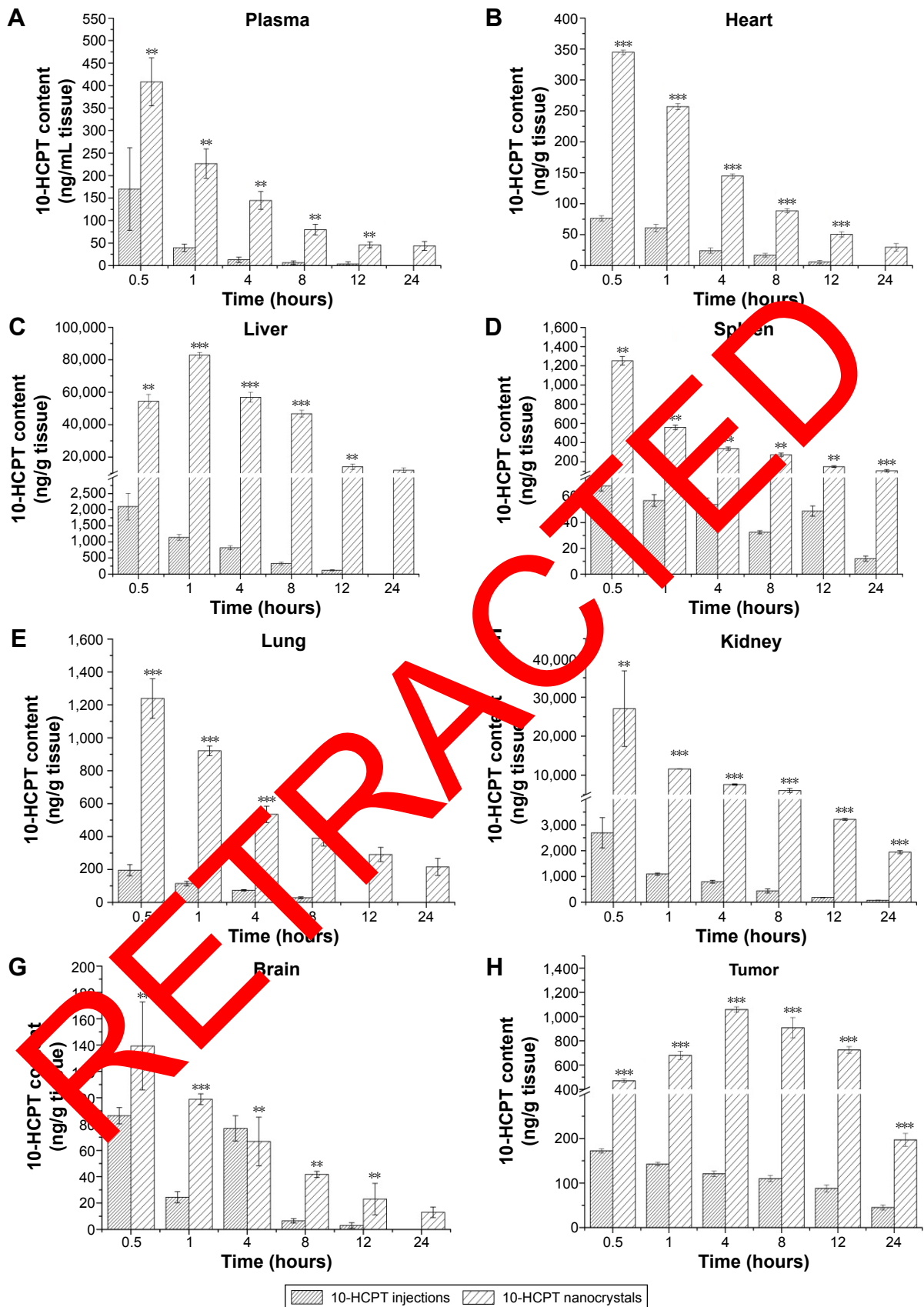


Figure 9 Tissue distribution of 10-HCPT in 4T1-bearing mice after an intravenous administration of 10-HCPT injections and 10-HCPT nanocrystals. **Notes:** 10-HCPT content changes in plasma (A), heart (B), liver (C), spleen (D), lung (E), kidney (F), brain (G) and tumor (H) after administration of 10-HCPT injections or nanocrystals. The dosage was 8.0 mg/kg, n=6. **P<0.01; ***P<0.001. **Abbreviation:** 10-HCPT, 10-hydroxycamptothecin.

Table 4 Comparison of parameters of tissue distribution of 10-HCPT injections and 10-HCPT nanocrystals in 4T1 bearing mice

Tissues	AUC _{0-24h} (ng·mL ⁻¹ ·h)		R _a	MRT/h		R _b	C _{max} (ng/mL)		R _c
	Inj	NCs		Inj	NCs		Inj	NCs	
Plasma	231.94	2,057.76	8.87	2.50	7.67	3.06	170.11	408.43	2.4
Heart	307.74	2,063.5	6.71	3.70	7.03	1.90	76.24	344.61	4.52
Liver	7,474.72	741,099.6	99.15	3.67	7.42	2.01	2,096.79	82,883.56	39.54
Spleen	918.20	5,717.57	6.23	9.10	7.79	0.86	68.52	1,251.99	18.27
Lung	690.09	9,284.85	13.45	3.56	8.71	2.44	195.28	1,238.95	6.34
Kidney	8,657.26	121,896.4	14.08	6.07	7.51	1.24	1,735.11	27,053.5	15.59
Brain	386.43	905.22	2.34	3.67	7.24	1.97	86.38	139.30	1.61
Tumor	2,172.00	15,747.17	7.25	9.41	9.09	0.97	172.23	1,057.96	6.14

Notes: R_a = AUC (NCs)/AUC (Inj); R_b = MRT (NCs)/MRT (Inj); R_c = C_{max} (NCs)/C_{max} (Inj).

Abbreviations: 10-HCPT, 10-hydroxycamptothecin; AUC_{0-24h}, area under the curve within 24 hours; C_{max}, peak concentration; Inj, injection; MRT, mean residence time; NCs, nanocrystals.

groups were all significantly less than those of the saline group, and the three 10-HCPT nanocrystals groups all showed significantly smaller tumor volumes than 10-HCPT injections group. The same trend was obvious in the tumor weights and the tumor inhibition rate data shown in Table 5. Judging merely by the tumor inhibition rate, a one-fourth dose, one-half dose, or the same dose of 10-HCPT nanocrystals could exhibit increasingly better in vivo antitumor effects (51.58% vs 37.93%, $P < 0.01$; 65.04% vs 37.93%, $P < 0.001$; 74.84% vs 37.93%, $P < 0.001$) compared with 10-HCPT injections. Together, these results showed that the nanocrystals could improve the antitumor efficacy of 10-HCPT injections.

Two main reasons contributed to these results. First, ~100% of 10-HCPT in the nanocrystals was in the lactone form, but the marketed injections were mainly in the carboxylate form.³³ and it is well known that the lactone form is more effective. On the other hand, the long-circulating

and slow-release forms of 10-HCPT nanocrystals along with the enhanced permeation and retention effect led to a greater accumulation of the drug in the tumor, as proved by the tissue distribution study.

The mouse survival and body weight growth data are usually used as indices to evaluate the side effects or toxicity of antitumor agents in in vivo pharmacodynamic experiments. As shown in Figure 11B, during the whole process of the 18-day treatment, one mouse in each of the four 10-HCPT groups died with the same survival rate of 90%, indicating similar toxicity among the groups. Figure 11C shows that a 1.25 mg/kg dose of 10-HCPT nanocrystals slightly increased the body weight compared with the 2.5 mg/kg dose of 10-HCPT nanocrystals, and the latter slightly increased the body weight compared with the 5 mg/kg dose of 10-HCPT injections by the end of the trial. However, there was no significant difference between the

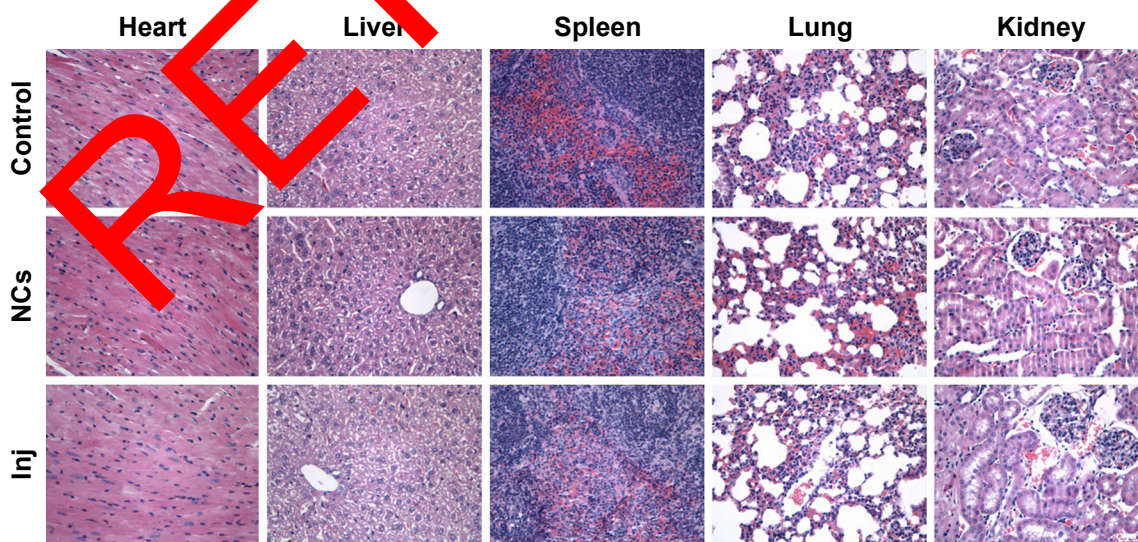


Figure 10 Histological analysis of the representative organs for control, 10-HCPT nanocrystals, and 10-HCPT injections groups (magnification, 400×).

Abbreviations: 10-HCPT, 10-hydroxycamptothecin; Inj, injections; NCs, nanocrystals.

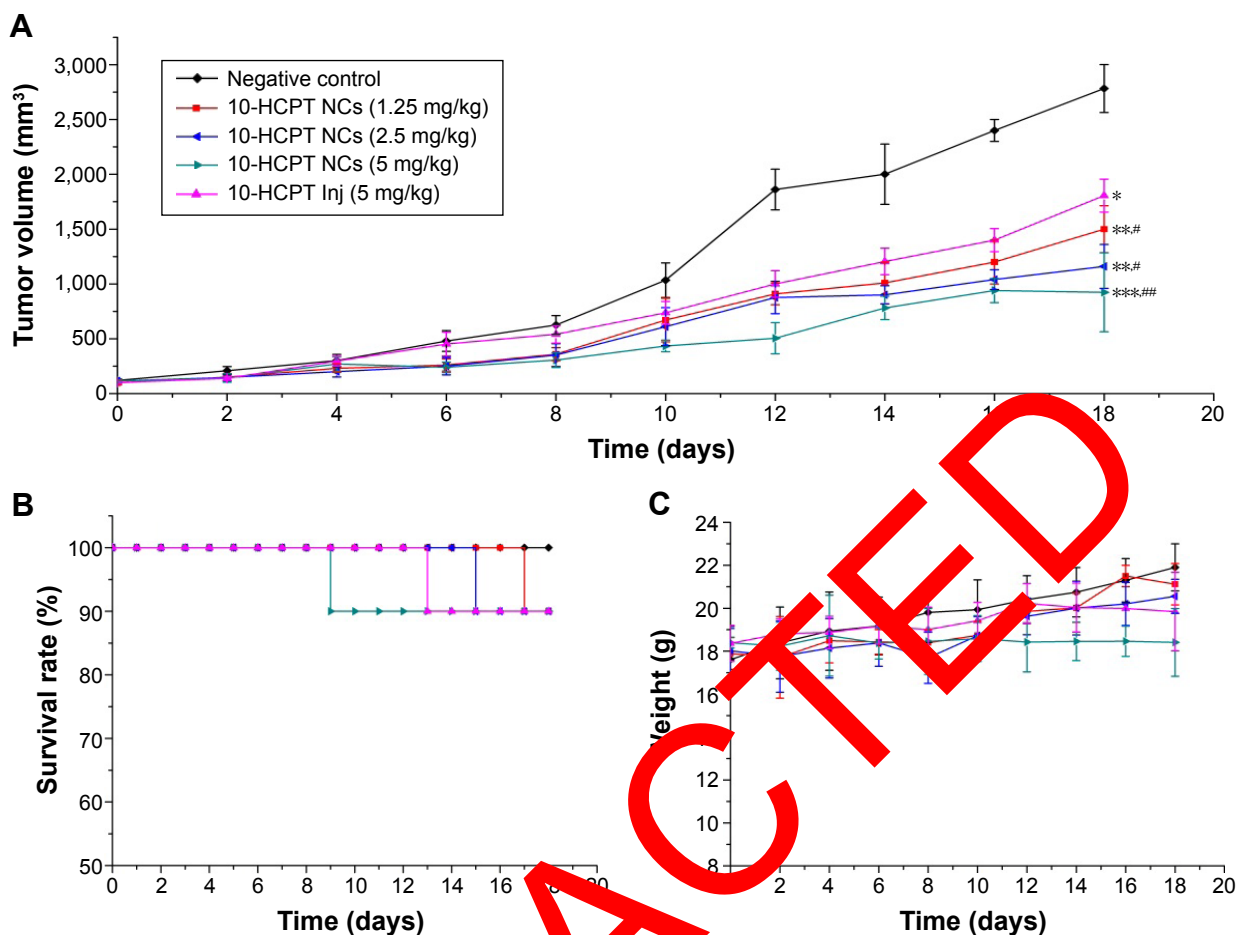


Figure 11 Changes in the parameters of 4T1-bearing mice after intravenous administration.

Notes: (A) Variations of tumor volume, (B) variations of survival, and (C) variations of body weights. $n=10$ or actual numbers. * $P<0.05$, ** $P<0.01$, and *** $P<0.001$ vs negative control; # $P<0.05$ and ### $P<0.01$ vs 10-HCPT Inj.

Abbreviations: 10-HCPT, 10-Hydroxycamptothecin; Inj, injection; NCs, nanocrystals.

three groups, indicating similar toxicity. In comparison, the body weight in mice receiving a 5 mg/kg dose of 10-HCPT nanocrystals was significantly reduced, indicating increased toxicity at this dose.

To sum up, it was believed that, at least at a half or a quarter dose, 10-HCPT nanocrystals could achieve improved therapeutic efficacy without increased side effects.

Table 5 The in vivo antitumor effects on 4T1-tumor bearing mice

Group	Tumor weight (g)	Inhibition (%)
Negative control	3.27±0.57	NA
10-HCPT injections (5 mg/kg)	1.98±0.38*	37.93
10-HCPT nanocrystals (1.25 mg/kg)	1.56±0.21*#	51.58
10-HCPT nanocrystals (2.5 mg/kg)	1.15±0.17*##	65.04
10-HCPT nanocrystals (5 mg/kg)	0.81±0.13*###	74.84

Notes: The tumor weight results are presented as mean ± SD, $n=6$. * $P<0.001$ vs negative control; # $P<0.01$, ### $P<0.001$ vs 10-HCPT injections.

Abbreviations: 10-HCPT, 10-hydroxycamptothecin; NA, not applicable; SD, standard deviation.

Conclusion

Through a modification of the acid–base microprecipitation combined with a high-pressure homogenization technique, a solvent-free, stabilizer-free, bottom–up method was successfully developed to prepare stable 10-HCPT nanocrystals with a small size and a high drug-loading capacity. It was proved that the resulting nanocrystals had a higher in vitro antiproliferative activity and cellular uptake than 10-HCPT injections.

10-HCPT nanocrystals exhibited much higher drug levels in the plasma and tissues of the test mice than the marketed 10-HCPT injections and significantly improved the antitumor therapeutic effect. In summary, this can be a promising drug delivery system with far-reaching applications.

Acknowledgments

This work was financially supported by the National Natural Science Foundation of China (Numbers U1401223, 30772659) and the China International Science and

Technology Cooperation Program for Key Projects (Number 2008DFA31070).

Disclosure

The authors report no conflicts of interest in this work.

References

- Wall ME. Camptothecin and taxol: discovery to clinic. *Med Res Rev.* 1998;18(5):299–314.
- Thomas CJ, Rahier NJ, Hecht SM. Camptothecin: current perspectives. *Bioorg Med Chem.* 2004;12(7):1585–1604.
- Rothenberg ML. Topoisomerase I inhibitors: review and update. *Ann Oncol.* 1997;8(9):837–855.
- Zhang X, Chen B. Recombinant high density lipoprotein reconstituted with apolipoprotein AI cysteine mutants as delivery vehicles for 10-hydroxycamptothecin. *Cancer Lett.* 2010;298(1):26–33.
- Kratz F, Abu Ajaj K, Warnecke A. Anticancer carrier-linked prodrugs in clinical trials. *Expert Opin Investig Drugs.* 2007;16(7):1037–1058.
- Shi K, Tian Y, Jiang YB, Wang L, Cui FD. Modified hydrolysis kinetics of the active lactone moiety of 10-hydroxycamptothecin by liposomal encapsulation. *Pharm Dev Technol.* 2010;15(6):644–652.
- Shi B, Fang C, Pei Y. Stealth PEG-PHDCA niosomes: effects of chain length of PEG and particle size on niosomes surface properties, in vitro drug release, phagocytic uptake, in vivo pharmacokinetics and antitumor activity. *J Pharm Sci.* 2006;95(9):1873–1887.
- Yang X, Li L, Wang Y, Tan Y. Preparation, pharmacokinetics and tissue distribution of micelles made of reverse thermo-responsive polymers. *Int J Pharm.* 2009;370(1–2):210–215.
- Zhu H, Cao J, Cui S, Qian Z, Gu Y. Enhanced tumor targeting and antitumor efficacy via hydroxycamptothecin-encapsulated folate-modified *N*-succinyl-*N'*-octyl chitosan micelles. *J Pharm Sci.* 2013;102(7):1318–1332.
- Zhang C, Ding Y, Yu LL, Ping Q. Polymeric micelle systems of hydroxycamptothecin based on amphiphilic *N*-alkyl-*N*-trimethyl chitosan derivatives. *Colloids Surf B Biointerfaces.* 2007;55(2):192–199.
- Hu W, Zhang C, Hu WJ, Fang Y, Hou WJ. Pharmacokinetic, tissue distribution, and the lactone/carboxylate equilibrium of hydroxycamptothecin delivered via aerosol in mice. *Int J Pharm.* 2010;83(7):1291–1298.
- Li Y, Wei P, Li J, Li L. Pharmacokinetic analysis and optimization of hydroxycamptothecin-loaded nanoparticles for liver targeting. *Drug Dev Ind Pharm.* 2012;38(7):837–847.
- Yang L, Cui F, Cun D, Tao S, Shi K, Lin W. Preparation, characterization and biodistribution of the lactone form of 10-hydroxycamptothecin (HCPT)-loaded bovine serum albumin (BSA) nanoparticles. *Int J Pharm.* 2007;340(1–2):163–170.
- Wang HD, Feng LE, Liu J, Chen Y, Jiang T, Xie Q. In vitro and in vivo anti-tumor efficacy of 10-hydroxycamptothecin lyomorphic nanoparticle dispersion: shape- and morph-dependent to toxicity and delivery of 10-hydroxycamptothecin to cancer cells. *Nanomedicine.* 2016;12(4):881–891.
- Suk JS, Xu Q, Kim J, Hanes J, Ensign LM. PEGylation as a strategy for improving nanoparticle-based drug and gene delivery. *Adv Drug Delivery Rev.* 2016;99(Pt A):28–51.
- Du J, Li X, Zhao H, et al. Nanosuspensions of poorly water-soluble drugs prepared by bottom-up technologies. *Int J Pharm.* 2015;495(2):738–749.
- Constantinides PP, Chaubal MV, Shorr R. Advances in lipid nanodispersions for parenteral drug delivery and targeting. *Adv Drug Deliv Rev.* 2008;60(6):757–767.
- Pu X, Sun J, Wang Y, et al. Development of a chemically stable 10-hydroxycamptothecin nanosuspensions. *Int J Pharm.* 2009;379(1):167–173.
- Kocbek P, Baumgartner S, Kristl J. Preparation and evaluation of nanosuspensions for enhancing the dissolution of poorly soluble drugs. *Int J Pharm.* 2006;312(1–2):179–186.
- Jiang YB, Sun WL, Wang W. Recrystallization and micronization of 10-hydroxycamptothecin by supercritical antisolvent process. *Ind Eng Chem Res.* 2012;51:2596–2602.
- Yang Z, Gong W, Wang Z, et al. A novel drug-polyethylene glycol liquid compound method to prepare 10-hydroxycamptothecin loaded human serum albumin nanoparticle. *Int J Pharm.* 2015;490:412–428.
- Zhao YX, Hua HY, Chang M, Li WJ, Zhang Y, Liu HM. Preparation and cytotoxic activity of hydroxycamptothecin nanosuspensions. *Int J Pharm.* 2010;392:64–71.
- Langer K, Balthasar S, Vogel V, Diener N, von Briesen H, Schubert D. Optimization of the preparation process for human serum albumin (HSA) nanoparticles. *Int J Pharm.* 2003;257(1–2):169–180.
- Wu G, Lai P, Wang ZB. The recent progress of poloxamer 188. *China Modern Doctor.* 2008;46:48–49.
- Sanchez A, Tobio M, Gonzalez L, Fabra A, Alonso MJ. Biodegradable micellar nanoparticles as long-term delivery vehicles for interferon- α . *Int J Pharm Sci.* 2003;18(3–4):221–229.
- Chen L, Wang Y, Zhang J, et al. Bexarotene nanocrystal-oral and parenteral formulation development, characterization and pharmacokinetic evaluation. *Eur J Pharm Biopharm.* 2014;87(1):160–169.
- Zaki M. Augmented cytotoxicity of hydroxycamptothecin-loaded nanoparticles in lung and colon cancer cells by chemosensitizing pharmaceutical excipients. *Drug Deliv.* 2014;21(4):265–275.
- Arias JL, Reddy LH, Couvreur P. Polymeric nanoparticulate system augmented the anticancer therapeutic efficacy of gemcitabine. *J Drug Target.* 2009;17(8):586–598.
- Yang LJ, Jiang JZ, Hong JY, et al. High Drug Payload 10-Hydroxycamptothecin nanosuspensions stabilised by Cholesterol-PEG: In Vitro and In Vivo Investigation [J]. *J Biomed Nanotechnol.* 2015;11(11):711–721.
- Zhao YX, Liu DX, Liang WQ, Ye ZW. In-vivo pharmacokinetics, tissue distribution and anti-tumour effect of hydroxycamptothecin delivered in oil-in-water submicron emulsions [J]. *J Pharm Pharmacol.* 2012;64(6):783–791.
- De Jong WH, Hagens WI, Krystek P, Burger MC, Sips AJ, Geertsma RE. Particle size-dependent organ distribution of gold nanoparticles after intravenous administration. *Biomaterials.* 2008;29(12):1912–1919.
- Kutscher HL, Chao P, Deshmukh M, et al. Enhanced passive pulmonary targeting and retention of PEGylated rigid microparticles in rats. *Int J Pharm.* 2010;402(1–2):64–71.
- Giovannella BC, Hinz HR, Kozielski AJ, Stehlin JS Jr, Silber R, Potmesil M. Complete growth inhibition of human cancer xenografts in nude mice by treatment with 20-(S)-camptothecin. *Cancer Res.* 1991;51(11):3052–3055.

International Journal of Nanomedicine

Publish your work in this journal

The International Journal of Nanomedicine is an international, peer-reviewed journal focusing on the application of nanotechnology in diagnostics, therapeutics, and drug delivery systems throughout the biomedical field. This journal is indexed on PubMed Central, MedLine, CAS, SciSearch®, Current Contents®/Clinical Medicine,

Submit your manuscript here: <http://www.dovepress.com/international-journal-of-nanomedicine-journal>

Dovepress

Journal Citation Reports/Science Edition, EMBASE, Scopus and the Elsevier Bibliographic databases. The manuscript management system is completely online and includes a very quick and fair peer-review system, which is all easy to use. Visit <http://www.dovepress.com/testimonials.php> to read real quotes from published authors.